Nonlinear State and Tire Force Estimation for Advanced Vehicle Control

Laura R. Ray

Abstract—**Vehicle motion and tire force histories are estimated from an incomplete, noise-corrupted measurement set using an extended Kalman filter. A nine degree-of-freedom vehicle model and an analytic tire force model are used to simulate true vehicle motion, and a five degree-of-freedom vehicle model is used in the estimator. The filtered histories of forces and motion can be used to construct tire force models through off-line analysis, and both tire force estimates and state estimates are available for real time control. No prior knowledge of tire force characteristics or external factors that affect vehicle motion is required for the nonlinear estimation procedure. Simulation of a simple slip control braking system using slip and slip angle estimates for feedback demonstrates the effectiveness of the extended Kalman filter in providing adequate state estimates for advanced control of ground vehicles.**

I. Introduction

KNOWLEDGE of the vehicle state and external tire forces is essential to determining the dynamic behavior of a vehicle and to designing automotive control systems that increase safety and improve handling characteristics. Tire forces that act during severe maneuvers are nonlinear with respect to wheel slip and wheel slip angles and cause a wide range of stability and handling properties. The forces also depend on uncontrollable external factors, such as road/tire interface properties, tire pressure and wear, and vehicle loads, that are difficult to sense or anticipate. Because direct sensing of tire forces, slip, slip angles, and external factors is an arduous task, vehicle control systems designed to maintain stability during emergencies typically follow rules based on extensive testing, rather than analytic control laws based on actual forces and accurate state estimates. Advanced control systems proposed for maintaining vehicle stability during severe maneuvers also require accurate tire force models and state estimates for feedback e.g., [1], [2]. Analytic tire force models such as that of [3] have been developed from combinations of machine tire testing and vehicle testing [4]. These models are adequate for simulation of advanced control systems, but they do not necessarily represent an actual vehicle fitted with a particular set of tires. Extensive testing is required to determine the parameters of an analytic model; it is inconceivable that parameters be determined for every potential tire, tire pressure, and wear state. Furthermore, the external factors that affect tire forces must be known in real-time in order to use analytic models for handling analysis and real-time control system design. State observers also depend on a tire force model. If the tire model assumed by the observer does not match that of the real vehicle, the observer may perform poorly or be unstable. Senger and Korturn [5] describe observers for the lateral dynamics of a vehicle that work well when tire forces are linear, but fail in the nonlinear range when either the road/tire interface properties or an accurate analytic tire force model is unknown. Normally, it is difficult to know either factor, and these observers have limited practical use.

Because knowledge of tire force characteristics and the vehicle state is vital to examining and controlling vehicle performance, a straightforward method of determining the forces and motion from sensor measurements is of paramount importance. In this paper, an extended Kalman filter (EKF) [6] is implemented to estimate the state and longitudinal and lateral tire force histories of a nine degree-of-freedom vehicle. Following the Estimation Before Modeling procedure [7], [8], regression analyses can be applied off-line to EKF data to construct a tire force model. Such a tire force model can be used to design advanced control systems and to determine vehicle handling characteristics. The EKF can also be implemented in real time to account for the external factors that influence tire forces and to provide real-time signals for feedback control. A slip control braking system that uses state estimate feedback is presented here to demonstrate the performance benefits of combined controller/estimator systems. Prior knowledge of road properties or tire parameters is not required to implement the EKF, and all sensors are contained on the vehicle (i.e., a fifth-wheel trolley is not needed). The ability to determine tire forces and state estimates in this manner has major implications on the analysis and control of all types of ground vehicles.

II. Nonlinear Estimation Procedure

The study described here consists of computer simulations of actual vehicle motion using a high-order, nonlinear vehicle model and an analytic tire force model, and subsequent state and force estimation using a lower order vehicle model with tire forces appended as state components to be estimated. Introducing "mismatch" between the true vehicle and the estimation model allows the simulation to approximate the analysis of data from a real vehicle. A nine degree-of-freedom bicycle model is used to simulate the true vehicle motion (Fig. 1). The model lumps the two front and rear wheels into a single front and rear wheel, neglecting roll motion, and it includes vertical (suspension) dynamics. Suspension dynamics in the true vehicle model retain the variation in the normal force that

Manuscript received October 13, 1993; revised October 11, 1994. Recommended by Guest Editor, G. Rizzoni.

L. R. Ray is with the Department of Mechanical Engineering, Christian Brothers University, 650 East Parkway, Memphis, TN 38104 USA.

IEEE Log Number 9408621.

would be present in an actual vehicle. The equations of motion are (and see (2) at the bottom of the page)

$$\begin{bmatrix} \dot{v}_x \\ \dot{v}_y \\ \dot{r} \\ \dot{\omega}_f \\ \dot{\omega}_r \end{bmatrix} = \begin{bmatrix} \frac{1}{m}[-F_{xf}\cos\delta_f - F_{yf}\sin\delta_f - F_{xr}] + v_y r \\ \frac{1}{m}[F_{yf}\cos\delta_f - F_{xf}\sin\delta_f + F_{yr}] + v_x r \\ \frac{1}{I_z}[L_f(F_{yf}\cos\delta_f - F_{xf}\sin\delta_f) - L_r F_{yr}] \\ \frac{1}{I_w}[F_{xf}R_w - K_b T_b] \\ \frac{1}{I_w}[F_{xr}R_w - (1-K_b)T_b] \end{bmatrix} \tag{1}$$

where, for small θ

$$\begin{bmatrix} dz_f \\ d\dot{z}_f \\ dz_r \\ d\dot{z}_r \end{bmatrix} = \begin{bmatrix} z_f - (z_s + L_f\theta) \\ \dot{z}_f - (\dot{z}_s + L_f\dot{\theta}) \\ z_r - (z_s - L_r\theta) \\ \dot{z}_r - (\dot{z}_s - L_r\dot{\theta}) \end{bmatrix} \tag{3}$$

The components of $\boldsymbol{x}(t) = [v_x\, v_y\, r\, \omega_f\, \omega_r\, z_s\, z_f\, z_r\, \theta]^T$ are longitudinal and lateral velocities, yaw rate, front and rear wheel angular velocities, sprung mass vertical displacement, front and rear wheel vertical displacement, and body pitch angle. $\boldsymbol{u}(t) = [\delta_f\, T_b]^T$ represents the front steer angle and applied braking torque. m is the total mass, I_z is the moment of inertia of the vehicle about its yaw axis, I_w is the moment of inertia of the wheel about its axle, and K_b is the fixed proportion of braking applied to the front wheel. The spring and damping constants in (2) are the lumped parameters associated with the passive suspension system and tires. Components of the force vector $\boldsymbol{F}(t) = [F_{xf}\, F_{xr}\, F_{yf}\, F_{yr}]$ are the front and rear longitudinal and lateral tire forces. Sign conventions for the forces and motion, and the remaining parameters in (1)–(3) are defined in Fig. 1. The analytic tire model of [3] is used to simulate the true tire forces $\boldsymbol{F}(t)$ in (1). This model generates longitudinal and lateral tire forces as a function of vehicle velocity, road coefficient of friction (μ), and normal tire force (F_z), given a set of tire parameters. Typical tire forces for fixed vehicle velocity, μ, and normal force are given in Fig. 2, as functions of slip and slip angle. Note that the analytic tire force model is used only to simulate the true vehicle motion. The estimation model has no knowledge of the true tire force characteristics.

The vehicle is subject to a Gaussian, white disturbance $\boldsymbol{w}(t) = [\dot{z}_{of}\, \dot{z}_{or}]^T$ due to road roughness and characterized by

$$E[\boldsymbol{w}(t)\,\boldsymbol{w}(\tau)^T] = AV(t)\boldsymbol{I}\delta(t-\tau) \tag{4}$$

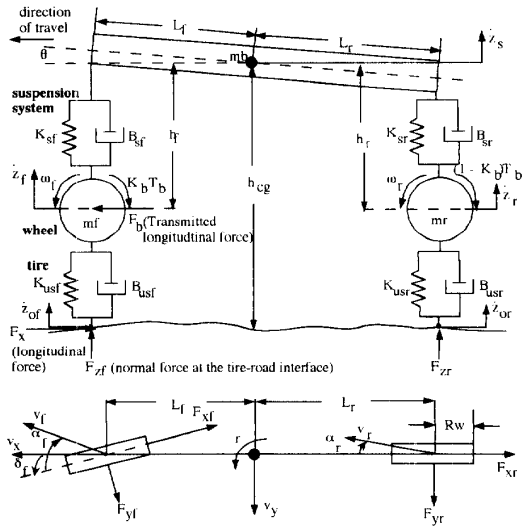

Fig. 1. Nine degree-of-freedom bicycle model: Schematic and sign conventions corresponding to (1) and (2).

where A characterizes the road roughness, V is the vehicle velocity, and $\boldsymbol{I}$ is a (2×2) identity matrix. For simplicity, the disturbance inputs are considered independent, and disturbances due to other factors are neglected. Equations (1)–(2) are integrated numerically, adding process noise characterized by (4), and measurement histories are constructed. The nonlinear measurement equation is

$$\boldsymbol{z}(t) = [r\,\omega_f\omega_r\, a_x\, a_y]^T = \boldsymbol{h}[\boldsymbol{x}(t),\, \boldsymbol{F}(t),\, \boldsymbol{u}(t))] + \boldsymbol{n}(t) \tag{5}$$

where a_x and a_y are the longitudinal and lateral accelerations, respectively, and $\boldsymbol{n}(t)$ is Gaussian, white measurement noise. In addition, it is assumed that the control inputs are measured. Measurements such as these are typically collected in test facilities to determine handling characteristics of a vehicle. Also, all sensors are contained on the vehicle, and the set includes readily available transducers, such as accelerometers, rate gyros, and tachometers.

An extended Kalman filter [6] is used to estimate the tire forces and vehicle state histories. The estimation model of the vehicle dynamics includes the first five equations of motion (1) and neglects suspension dynamics (2) in order to keep the size of the estimation model and the sensing requirements to a minimum. The state vector $\boldsymbol{x}(t)$ is augmented to include differential equations for each force to be estimated. Following [8], an integrated random walk is chosen to model each force,

$$\begin{bmatrix} \ddot{z}_s \\ \ddot{z}_f \\ \ddot{z}_r \\ \ddot{\theta} \end{bmatrix} = \begin{bmatrix} \frac{1}{m_b}[K_{sf}\,dz_f + B_{sf}\,d\dot{z}_f + K_{sr}\,dz_r + B_{sr}\,d\dot{z}_r] \\ \frac{1}{m_f}[K_{usf}(z_{of} - z_f) + B_{usf}(\dot{z}_{of} - \dot{z}_f) - K_{sf}\,dz_f - B_{sf}\,d\dot{z}_f] \\ \frac{1}{m_r}[K_{usr}(z_{or} - z_r) + B_{usr}(\dot{z}_{or} - \dot{z}_r) - K_{sr}\,dz_r - B_{sr}\,d\dot{z}_r] \\ \frac{1}{I_p}[-F_{bf}h_f\cos\delta_f - F_{br}h_r + L_f(K_{sf}\,dz_f + B_{sf}\,d\dot{z}_f) - L_r(K_{sr}\,dz_r + B_{sr}\,d\dot{z}_r)] \end{bmatrix} \tag{2}$$

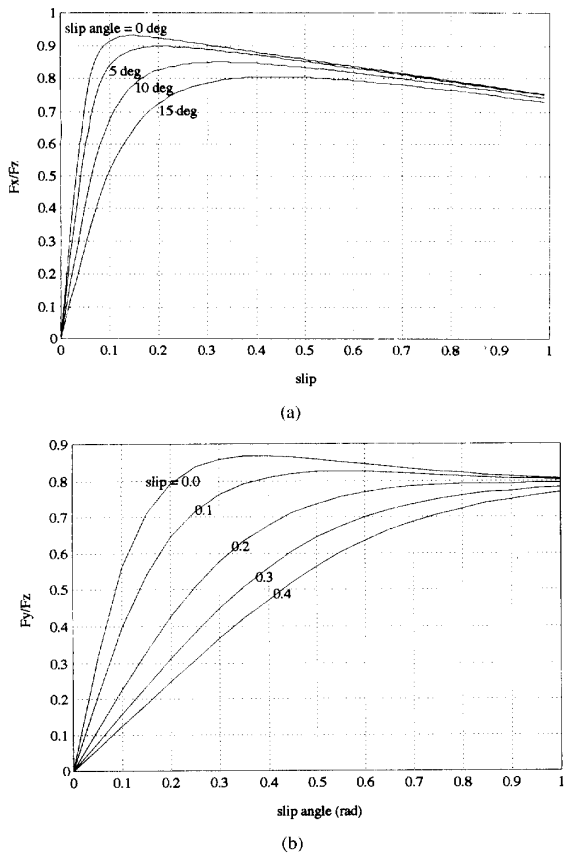

Fig. 2. Tire force curves for $F_z = 8000$ N, $\mu = 0.85$, $v_x = 25$ m/s. (a) Longitudinal force vs. slip for $0 \leq \alpha \leq 15$ deg. (b) Lateral force vs. slip angle for $0 \leq$ slip ≤ 0.4.

allowing the forces to vary with time as necessary

$$\begin{bmatrix} \dot{y}_0 \\ \dot{y}_1 \\ \dot{y}_2 \end{bmatrix} = \begin{bmatrix} 0 & 1 & 0 \\ 0 & 0 & 1 \\ 0 & 0 & 0 \end{bmatrix} \begin{bmatrix} y_0 \\ y_1 \\ y_2 \end{bmatrix} + \boldsymbol{w}_y \tag{6}$$

y_0 represents the force to be estimated, y_1, y_2 are first and second time derivatives of the force, and $\boldsymbol{w}_y$ is random, white noise. (Other second and third-order Gauss-Markov models were evaluated, and good results were obtained for a variety of models.) Equation (6) is appended to the estimator state equations for each of the four forces, resulting in a 17th-order estimation model. Denoting the estimated variables as $\hat{(\cdot)}$ and the nonlinear function of (1) as $\boldsymbol{f}(\boldsymbol{x}(t), \boldsymbol{F}(t), \boldsymbol{u}(t))$, the augmented nonlinear differential equation that models the system in the state estimator is

$$\dot{\hat{\boldsymbol{x}}}_{\boldsymbol{A}}(t) = \begin{bmatrix} \dot{\hat{\boldsymbol{x}}}(t) \\ \dot{\hat{\boldsymbol{F}}}(t) \end{bmatrix} = \begin{bmatrix} \boldsymbol{f}(\hat{\boldsymbol{x}}(t), \hat{\boldsymbol{F}}(t), \boldsymbol{u}(t)) \\ \boldsymbol{A}\hat{\boldsymbol{F}}(t) \end{bmatrix} = \boldsymbol{f}_{\boldsymbol{A}}(\hat{\boldsymbol{x}}_{\boldsymbol{A}}(t), \boldsymbol{u}(t)) \tag{7}$$

$$\hat{\boldsymbol{y}}(t) = \boldsymbol{h}_{\boldsymbol{A}}(\hat{\boldsymbol{x}}_{\boldsymbol{A}}(t), \boldsymbol{u}(t) \tag{8}$$

where $\boldsymbol{A}$ is a block-diagonal matrix with blocks defined by the matrix in (6), $\hat{\boldsymbol{x}}_{\boldsymbol{A}}(t)$ is the augmented state vector, and $\hat{\boldsymbol{y}}(t)$ is the output reconstructed based on the estimation model and the state estimate. The discrete-time extended Kalman filter is implemented by integrating (7) and its corresponding continuous-time matrix Riccati equation from time t_{k-1} to time t_k to propagate the state and error covariance ($\boldsymbol{P}$) estimates (9) and (10), computing the filter gain matrix (11), and updating the state and covariance estimates based on the measurement residual (12) and (13) [6]

$$\hat{\boldsymbol{x}}_{\boldsymbol{A}_k}(-) = \hat{\boldsymbol{x}}_{\boldsymbol{A}_{k-1}}(+) + \int_{t_{k-1}}^{t_k} \boldsymbol{f}_{\boldsymbol{A}}(\hat{x}_{\boldsymbol{A}}(\tau), \boldsymbol{u}(\tau))\, d\tau \tag{9}$$

$$\boldsymbol{P}_k(-) = \boldsymbol{P}_{k-1}(+) + \int_{t_{k-1}}^{t_k} \{\boldsymbol{F}(\tau)\boldsymbol{P}(\tau) + \boldsymbol{P}(\tau)\boldsymbol{F}^T(\tau) + \boldsymbol{L}\boldsymbol{A}\boldsymbol{V}(\tau)\boldsymbol{L}^T\}\, d\tau \tag{10}$$

$$\boldsymbol{K}_k = \boldsymbol{P}_k(-)\boldsymbol{H}_k^T[\boldsymbol{H}_k\boldsymbol{P}_k(-)\boldsymbol{H}_k^T + \boldsymbol{R}_k]^{-1} \tag{11}$$

$$\hat{\boldsymbol{x}}_{\boldsymbol{A}_k}(+) = \hat{\boldsymbol{x}}_{\boldsymbol{A}_k}(-) + \boldsymbol{K}_k[\boldsymbol{z}_k - h_{\boldsymbol{A}}(\hat{\boldsymbol{x}}_{\boldsymbol{A}_k}(-), \boldsymbol{u}(t))] \tag{12}$$

$$\boldsymbol{P}_k(+) = [\boldsymbol{I} - \boldsymbol{K}_k\boldsymbol{H}_k]\boldsymbol{P}_k(-). \tag{13}$$

Matrices $\boldsymbol{F}$ and $\boldsymbol{H}$ are computed by linearizing (7)–(8) around $\hat{\boldsymbol{x}}_{\boldsymbol{A}_k}(-)$ at each time step. The disturbance input matrix, $\boldsymbol{L}$, is constant, since the disturbances enter linearly. The equations governing the tire forces in the estimation model are driven by the measurement residual $[\boldsymbol{z}_k - \boldsymbol{h}(\hat{\boldsymbol{x}}_{\boldsymbol{A}_k}(-), \boldsymbol{u}(t))]$ in (12). The filter is initialized with a state estimate corresponding to the true state and a large covariance matrix.

Slip and slip angle estimates are derived from the state estimate. Estimates of the front and rear wheel slip angles (α) and longitudinal slip (s) are given by

$$\hat{\alpha}_f = \delta_f - \tan^{-1}\left[\frac{\hat{v}_y + L_f\hat{r}}{\hat{v}_x}\right], \tag{14}$$

$$\hat{\alpha}_r = -\tan^{-1}\left[\frac{\hat{v}_y - L_r\hat{r}}{\hat{v}_x}\right] \tag{15}$$

$$\hat{s}_f = 1 - \frac{\hat{\omega}_f R_w}{\hat{v}_f \cos\hat{\alpha}_f}, \tag{16}$$

$$\hat{s}_r = 1 - \frac{\hat{\omega}_r R_w}{\hat{v}_r \cos\hat{\alpha}_r} \tag{17}$$

where $\hat{v}_f$ and $\hat{v}_r$ are the estimated magnitudes of the front and rear axle velocities, respectively

$$\hat{v}_f = \sqrt{(\hat{v}_y + L_f\hat{r})^2 + \hat{v}_x^2}, \tag{18}$$

$$\hat{v}_r = \sqrt{(\hat{v}_y - L_r\hat{r})^2 + \hat{v}_x^2}. \tag{19}$$

III. Evaluation of the Extended Kalman Filter

A combined steering and braking maneuver is simulated on a road surface with a sudden reduction in μ, for evaluation of the EKF. The control inputs and small coefficient of friction are severe enough to cause wheel slips and slip angles in the nonlinear regime of the tire force curves of Fig. 2. Vehicle parameters and filter parameters are given in Table I. State and force estimates are presented in Fig. 3 for the maneuver considered. The controls $T_b = 2000$ N-m, $\delta f = 0.05$ rad are applied at $t = 0$ sec, and at $t = 0.6$ sec, μ changes from 0.85 to 0.3. Although the change in μ is unknown to the estimator, the state and tire force estimates are very good. The state estimate follows the actual state very closely, and the

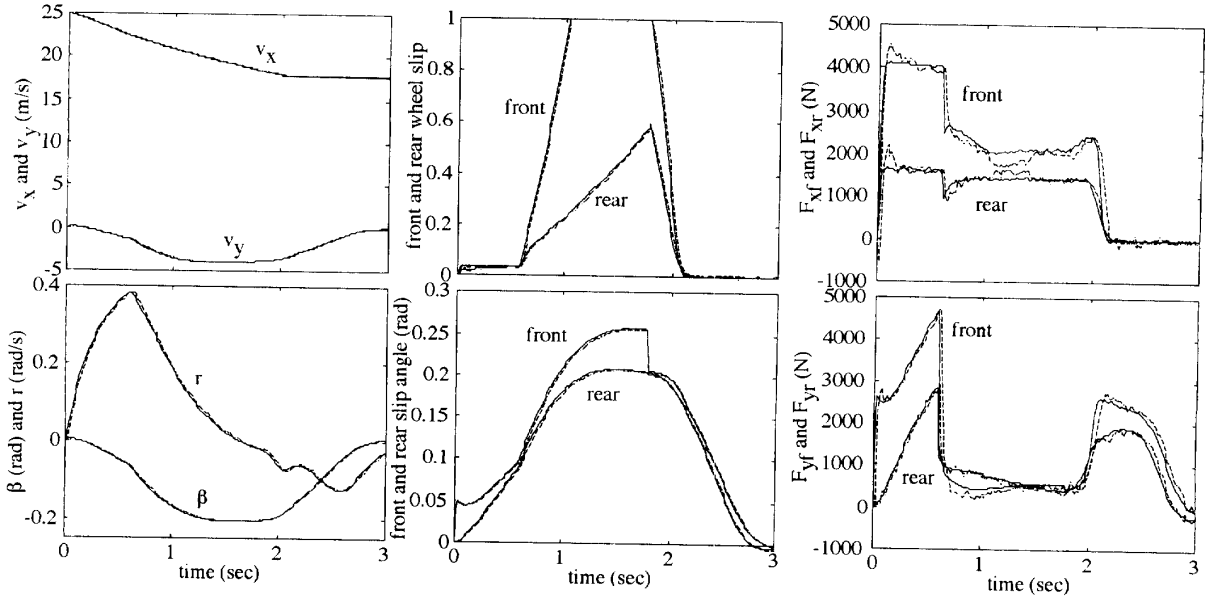

Fig. 3. Actual motion (solid lines) and state estimates (dashed lines) for $T_b = 2000$ N-m, $\delta f = 0.05$ rad applied at $t = 0$ on a road surface with $\mu = 0.85$. At 0.6 sec, the coefficient of friction changes to $\mu = 0.3$, and at 1.8 sec, the braking and steering controls are removed.

TABLE I
SIMULATION PARAMETERS

Parameter	Value	Parameter	Value
m	1301 kg	K_{usf}	30000 N/m
m_b	1171 kg	K_{usr}	30000 N/m
m_f	70 kg	B_{usf}	80 N-s/m
m_r	60 kg	B_{usr}	80 N-s/m
L_f	1.0 m	K_{sf}	30000 N/m
L_r	1.45 m	K_{sr}	35000 N/m
I_z	1627 kg-m	^{2} B_{sf}	5000 N/m
h_{cg}	0.53 m	B_{sr}	4500 N/m
R_w	0.33 m	I_p	2035 kg-m^2
I_w	4.07 kg-m	K_b	K_b

Extended Kalman Filter parameters
R_k = diag [1E-5 0.1 0.1 0.1 0.01 0.01], A = 4.8E-6 m
Sample time, T = 0.01 to 0.03 sec

force estimates follow the true force histories closely after an initial transient. When the controls are removed at $t = 1.8$ sec, estimator performance remains good after transients settle.

IV. CONSTRUCTING A TIRE FORCE MODEL

The method proposed to construct nonlinear tire force curves such as those in Fig. 2 stems from a comparable problem associated with aircraft dynamics. The EBM technique described and used in [7], [8] has been successfully applied to determine the aerodynamic forces and moments acting on an aircraft as a function of the aircraft state (e.g., velocity and angle-of-attack). Aerodynamic forces and moments are, like tire forces, nonlinear as a function of the angle-of-attack. In EBM, the EKF is followed by a smoother to estimate smooth histories of the vehicle state and forces; the smoother acts on the entire measurement histories in post-processing of data. Subsequently, regression analyses are applied to smoothed histories to determine the aerodynamic forces as functions of the state and control vectors. While a smoother can improve EKF estimates, it is not used in this study. Instead, the filtered estimates provide data directly for regression analyses. The results presented here show the data that would be available from filtering without actually performing the regressions.

Equations (1)–(2) are coupled through the variation in normal force at the tire/road interface due to the disturbance. In the true vehicle model, the normal force depends on suspension dynamics; since the estimation model does not retain the suspension dynamics, a static approximation of the normal force is made in order to produce a tire force model normalized by F_z, such as that of Fig. 2. The static normal force approximation at the front and rear wheels, respectively, is

$$F_{zf} = \frac{m_b g L_r - m_b a_x h_{cg}}{L_f + L_r} + m_f g, \tag{20}$$

$$F_{zr} = \frac{m_b g L_f + m_b a_x h_{cg}}{L_f + L_r} + m_r g \tag{21}$$

where $g = 9.8$ m/s^2. F_{zf} and F_{zr} are estimated using the vehicle parameters in Table I and the measured value of longitudinal acceleration.

Single input maneuvers provide the data necessary to construct tire force curves. Fig. 4 shows the true and estimated slip and force histories for pure braking, with $T_b = 4000$ N-m. The corresponding steady-state deceleration is $a_x = -8.4$ m/sec^2, and there is no lateral motion (v_y, r, F_{yf}, F_{yr}, and slip angles are zero) in the absence of lateral disturbances. These data can be used to produce longitudinal force vs. slip curves at zero slip angle and constant normal force. The normal force histories also are given in Fig. 4; the unknown actual normal force undergoes a transient and varies substantially due to suspension dynamics, while the static approximation is constant after the

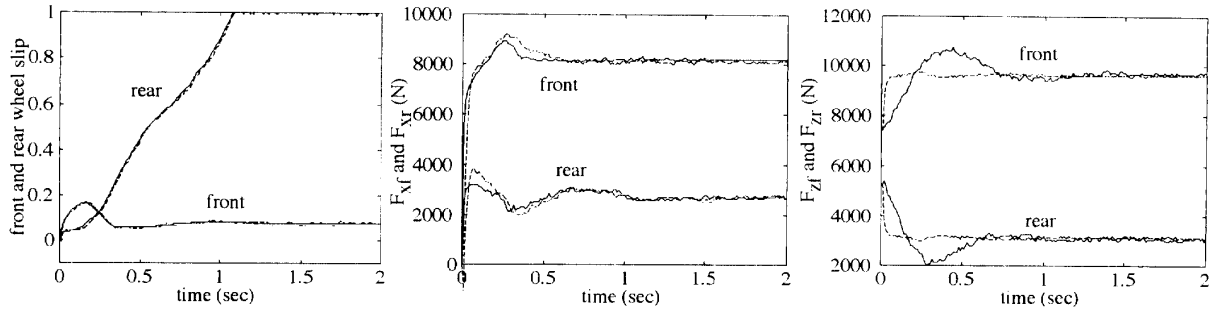

Fig. 4. Actual (solid) and estimated (dashed) slip and force estimates for $T_b = 4000$ N-m, $\mu = 0.85$, for entire trajectory. The normal force curves show the actual normal forces and the static approximations.

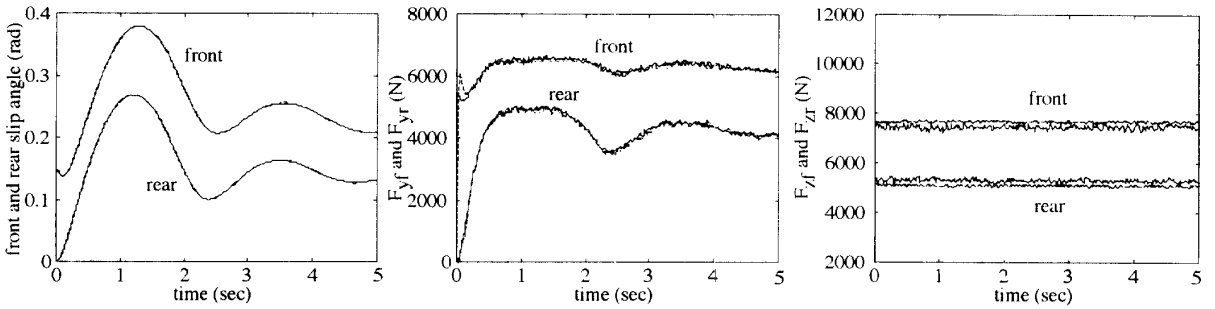

Fig. 5. Actual (solid) and estimated (dashed) slip angle and force estimates for $\delta f = 0.15$ rad, $\mu = 0.85$, for entire trajectory.

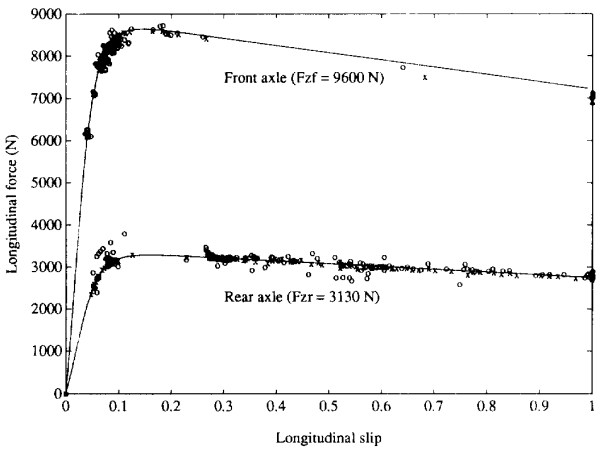

Fig. 6. Regression data for per-axle normal forces $F_{zf} = 9600 \pm 50$ N, $F_{zr} = 3130 \pm 50$ N, and $\alpha = \pm 0.5$ deg. 'x' represents actual force vs. slip data, and 'o' represents data derived from state estimates. The solid line represents the true tire force curve for fixed velocity and normal force.

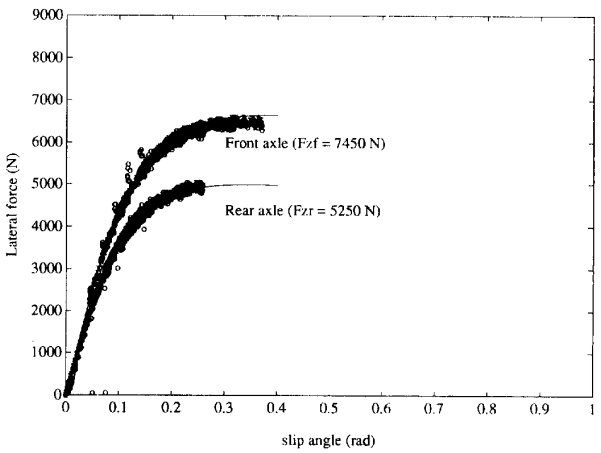

Fig. 7. Regression data for per-axle normal forces $F_{zf} = 7450 \pm 30$ N, $F_{zr} = 5250 \pm 30$ N, and s = ± 0.01. 'x' represents actual data, and 'o' represents data derived from state estimates. The solid line represents the true tire force curve for fixed velocity and normal force.

initial acceleration transient. Fig. 5 shows estimated slip angle and lateral force histories for a pure steering maneuver with $\delta f = 0.15$ rad. Here, the variables associated with longitudinal motion (a_x, F_{xf}, F_{xr}, and slip ratios) remain small but are non zero due to the disturbance. Note that the initial front slip angle is 0.15 rad, corresponding to the steering input. These histories provide data for lateral force vs. slip angle curves at zero slip and approximately constant normal force. Carefully chosen maneuvers that combine steering and braking for a range of inputs can provide data required to construct a family of tire force curves such as in Fig. 2.

Filtered slip, slip angle, and force histories such as those of Figs. 4 and 5 serve as inputs to a regression analysis that determines the per-axle tire forces as functions of normal force, slip, and slip angle. First, state estimates are computed for a range pure braking or pure steering maneuvers in the nonlinear tire force regime. The resulting force histories are sorted into sets with specified normal force and slip angle or slip range. A least-squares or other algorithm can be used to fit a polynomial function of slip to each set of data e.g., [9]. Figs. 6 and 7 present the kind of data that would be available for regression. Braking maneuvers from $T_b = 1000$

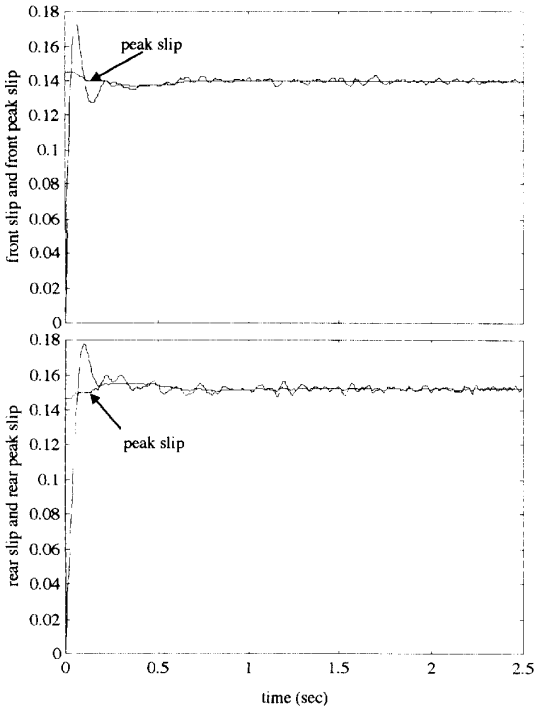

Fig. 8. Front and rear slip histories and peak slip histories for the "Ideal" slip control braking system for a severe longitudinal braking maneuver: PI controller is based on feedback of a perfect slip signal and seeks to control slip at the peak slip value.

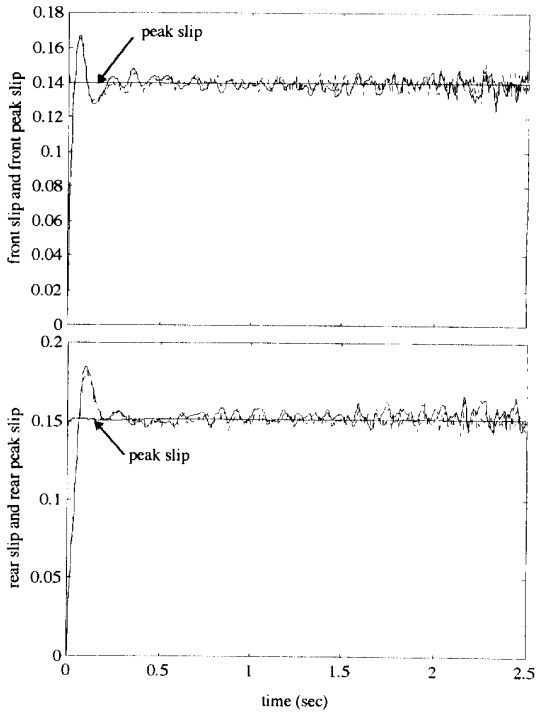

Fig. 9. Front and rear slip histories (solid), slip estimates (dashed), and peak slip histories of the PI/EKF system for a severe longitudinal braking maneuver: PI controller is based on feedback of a slip estimates from EKF and seeks to control slip at the peak slip value.

to 5000 N-m are simulated to produce the data for slip vs. longitudinal force at zero slip angle shown in Fig. 6. The solid line shows the analytic tire force curve for the given normal force and maximum vehicle velocity. "Outliers" are attributed to transients in the force estimate histories, disturbances, measurement noise, and differences between actual normal force and the static approximation during the initial transient. Data provided by the EKF reconstruct the tire model reasonably well. Note that only a few points are available in the linear region of the tire force curve since data are derived from severe braking. Also, few points are available for F_{xf} vs slip since the front wheel does not lock for the range of applied braking and resulting normal force considered. Pure steering maneuvers from $\delta f = 0.05$ to 0.15 rad are simulated to produce regression data for slip angle vs. lateral force at approximately zero slip shown in Fig. 7. Data for the front axle are available only for higher values of slip angle, since the steering input contributes directly to the slip angle. Outliers are again attributed to transients, noise, and differences between the actual normal force and the static approximation.

V. Braking Control Using Slip Estimate Feedback

A number of researchers have shown that slip control braking systems (SCBS) provide significant reductions in stopping distances and improvement in vehicle stability during lateral maneuvers e.g., [1], [2]. These systems generally require knowledge of the road coefficient of friction, a tire force model, peak slip (slip associated with the peak longitudinal force), and slip and slip angle signals for feedback. During braking, if slip can be controlled to the value corresponding to maximum longitudinal force, stopping distance can be minimized. Here, a simple proportional-integral (PI) slip control braking system is implemented to assess achievable performance of control systems designed using slip estimate feedback. The emphasis of this example is not on the control system design, but on the ability to implement a given control system by providing the signals required for feedback using extended Kalman filtering. In this example, it is assumed that a nominal tire force model exists and the road coefficient of friction is known, so that peak slip can be identified. Such a tire force model can be constructed experimentally using the methods outlined in this paper. Real time identification of μ is the subject of future research; it is conceivable that μ can be determined during a braking maneuver by identifying, in real time, the portion of a tire force model governing vehicle motion [10]. μ is required only to determine the setpoint for the slip controller; the EKF still requires no knowledge of μ or the tire force model.

The proportional-integral slip control braking system that uses state estimates from extended Kalman filtering for feedback will be called the PI/EKF system. The performance of this system is compared to an "Ideal" PI slip control braking system, where slip is measured without error and peak slip is known without error. The Ideal PI system gives the best

possible performance for the given PI controller. While it is assumed that the true value of peak slip is known for the Ideal system, the PI/EKF system chooses peak slip based on road coefficient of friction, normal force estimates, and the tire force model. The PI slip control law is given by

$$u(t) = K_p e(t) + Ki \int_0^t e(t)\,dt \tag{22}$$

where $K_p = 13000$ N-m and $K_i = 3000$ N-m/s are the proportional and integral control gains, $u(t)$ is the applied braking torque, and $e(t)$ is the error between the peak slip and the actual slip. It is assumed that braking of each axle of the vehicle is controlled independently (i.e., K_b is not constant), and the peak slip may differ for each axle. The control gains are the same for each axle. For simplicity, no control dynamics or driver models are included. The control system is activated during severe braking, when the applied torque would cause wheel lock of one or both axles. Peak slip is determined at each time step; the actual value of peak slip may exhibit a transient due to the normal force transient. During pure longitudinal braking, peak slip is the value corresponding to maximum longitudinal force when both front and rear slip angles are zero. During combined steering and braking maneuvers, peak slip is defined as that value corresponding to maximum longitudinal force when slip angle is equal to df (the steering input) and zero, respectively, for the front and rear axles.

Fig. 8 shows the front and rear slip signals and slip setpoints of the Ideal system for straight-line braking from 29 m/s on a road surface with $\mu = 0.85$, and Fig. 9 shows slips, slip estimates, and slip setpoints of the PI/EKF system for the same maneuver. The results show that controller is able to maintain slip setpoints using slip estimate feedback, and state estimate feedback produces little performance degradation. At the end of the three second trajectory, both systems have a longitudinal displacement of 46.5 m, and longitudinal velocities are 1.9 m/s and 2.2 m/s, respectively. The average longitudinal acceleration is $-9.05\,\mathrm{m/s^2}$ for both the Ideal system and the PI/EKF system.

The phase plot of a combined 0.15 rad steering and severe braking maneuver is given in Fig. 10 for each case. Again, the PI/EKF system performs almost identically to the ideal system. The longitudinal displacement, lateral displacement, and velocity at the end of the maneuver are 48.2 m, 5.7 m, and 3.3 m/s, respectively, for the Ideal system, and 48.2 m, 5.8 m, and 3.4 m/s for the PI/EKF system. Fig. 11 shows the PI/EKF front and rear slip histories along with their respective setpoints, and Fig. 12 compares longitudinal and lateral accelerations of the Ideal and PI/EKF systems. Again, the PI/EKF system shows no significant performance degradation over the Ideal system.

VI. Real Time Implementation of the Extended Kalman Filter

Approximately 134,000 floating point operations (FLOPS) per sample time are performed in the EKF (without modification of the EKF for computation efficiency). Based on current processor speeds of 5 to 20 MFLOPS/sec [11], filter computations can be performed in 0.007 to 0.027 seconds. Modification of numerical integration routines for computational efficiency can reduce the number of floating point operations by a factor of two. Simulation sample times of 0.01–0.03 sec were used without incurring numerical difficulties, indicating that real-time implementation of the 17th order EKF would be possible using current technology.

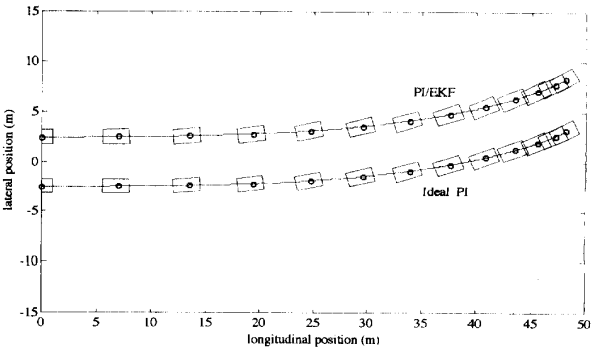

Fig. 10. Phase trajectory of the Ideal system and the PI/EKF system for a combined steering and braking maneuver.

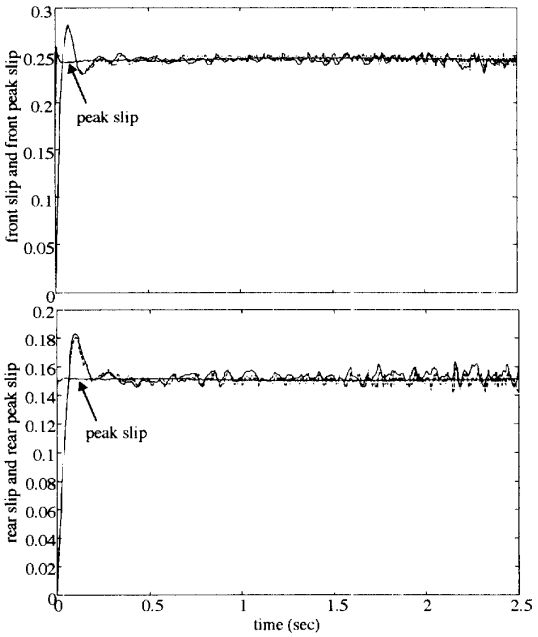

Fig. 11. Front and rear slip histories (solid), slip estimates (dashed), and peak slip histories of the Ideal system and the PI/EKF system for a combined steering and braking maneuver.

VII. Conclusions

Preliminary analyses show that extended Kalman filtering provides good estimates of vehicle motion and tire force histories. Using a simulation based on the nine degree-of-freedom vehicle and an analytic tire force model, normal and severe maneuvers combining steering, braking, and varying road conditions were simulated. The estimated state and tire force histories follow the actual state and force histories

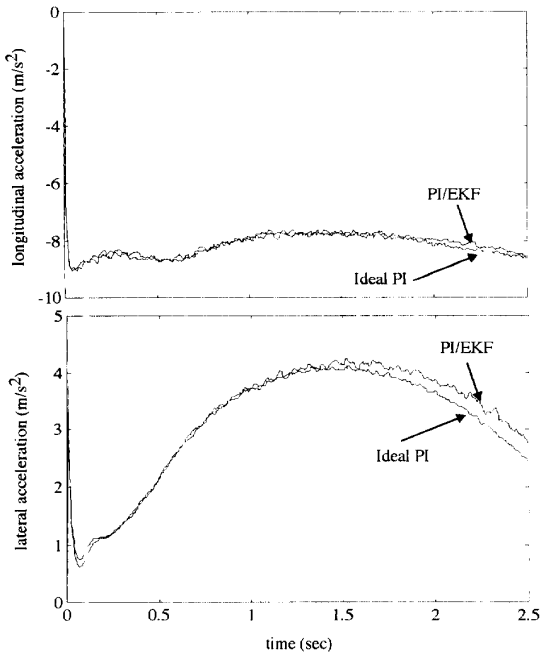

Fig. 12. Longitudinal and lateral accelerations of the Ideal system and the PI/EKF system for a combined steering and braking maneuver.

well, even with mismatch between the true vehicle and the estimation model. Carefully selected maneuvers provide data that can be used to construct tire force models in both the linear and nonlinear regime. Prior knowledge of the road/tire interface properties, tire pressures, or tire model is not required to use the proposed technique, and sensor requirements are reasonable. When the estimator is combined with a simple PI slip control braking system, the system showed little performance degradation from stopping distances that are achievable if slip could be measured without error for feedback. Computation requirements suggest that the EKF can be implemented in real time; hence, it is conceivable that the vehicle state and force estimates would be available as control signals. As a result, controllers such as that demonstrated, that have not been practical previously, may be useful in the future to enhance vehicle stability and performance.

REFERENCES

[1] S. Taheri and E. H. Law, "Investigation of a combined slip control braking and closed loop four wheel steering system for an automobile during combined hard braking and severe steering," *Proc. 1990 American Control Conference*, San Diego, CA, 1990.

[2] S. Kimbrough, "A brake control strategy for emergency stops that involve steering," *Proc. ASME Symp. Transportation Sys.*, Dallas Texas, pp. 117–129, Nov. 1990.

[3] H. T. Szostak, R. W. Allen, and T. J. Rosenthal, "Analytical modeling of a driver response in crash avoidance maneuvering, Vol. II: An interactive tire model for driver/vehicle simulation," U.S. Department of Transportation, report no. DOT HS 807-271, Apr. 1988.

[4] R. W. Allen, H. T. Szostak, T. J. Rosenthal, and D. E. Johnston, "Test methods and computer modeling for the analysis of ground vehicle handling," *Society Automotive Engineers*, Paper no. 861115.

[5] K. H. Senger and W. Korturn, "Investigations on state-observers for the lateral dynamics of four-wheel steered systems," *The Dynamics Vehicles on Roads and Tracks: Proc. 11th IAUSD Symp. Dynamics Vehicles Roads Tracks*, pp. 515–517, Aug. 1989.

[6] R. F. Stengel, *Stochastic Optimal Control: Theory and Application*. New York: John Wiley and Sons, 1986.

[7] H. L. Stalford, "High-alpha aerodynamic model identification of T-2C aircraft using the EBM method," *J. Aircraft*, vol. 18, no. 10, pp. 801–809, Oct. 1981.

[8] M. Sri-Jayantha and R. F. Stengel, "Determination of nonlinear aerodynamics coefficients using the estimation-before-modeling method," *J. Aircraft*, vol. 25, no. 9, pp. 796–804, Sept. 1988.

[9] A. Sitchin, "Acquisition of transient tire force and moment data for dynamic vehicle handling simulations," *SAE Trans.*, sect. 4, paper no. 831790, pp. 1098–1110, 1983.

[10] L. R. Ray, "Real-time determination of road coefficient of friction for IVHS and advanced vehicle control," in *Proc. 1995 Amer. Contr. Conf.*, Seattle, WA, to appear June 1995.

[11] Texas Instruments Incorporated, private communication, Feb 1992.

Laura R. Ray received the B.S.E. and Ph.D. degrees in mechanical and aerospace engineering from Princeton University in 1984 and 1991, respectively. From 1990 to 1992 she was a Faculty Member of the Mechanical Engineering Department at Clemson University, and she has been a Faculty Member of the Mechanical Engineering Department at Christian Brothers University since 1993. Her current research interests include applications of control theory to automotive, air transportation, and robotic systems, control system robustness, computer-aided control system design, and IVHS.